Palestine Journal of Mathematics

Vol 14 (Special Issue IV), (2025) , 53–66

EFFECT OF INCLINED LOAD ON PLANE WAVE IN NONLOCAL THERMOELASTIC THREE-PHASE LAG MODEL

S. Bajaj, A. K. Shrivastav and S. Kumari

2010 Mathematics Subject Classification: 74J15, 74F05.

Keywords and phrases: Inclined load, nonlocal, three-phase lag model, thermoelastic model.

We sincerely thank the reviewers and the editor for their insightful comments and helpful suggestions, which have significantly enhanced the quality of our manuscript.

Abstract The main aim of this research article is to study the effect of inclined load and nonlocality on the plane wave in the context of three-phase lag thermoelastic media. The governing equation of a plane wave in a three-phase lag thermo-elastic model is solved numerically by the normal mode analysis technique. The numerical results are calculated in terms of temperature, stress, and displacement with the effect of nonlocal parameter. The graphic presentation of the results shows the evident effect of phase lag, non-locality, and tilt angle. The physical properties of the magnesium crystal-like material are used for numerical simulations.

1 Introduction

Thermoelasticity deals with the mechanical behavior of materials governed by a linear relationship between stress and strain under non-isothermal conditions. The mechanical and thermal field domains studied under thermoelasticity significantly affect the contraction and expansion of the elastic material. This includes the effect on temperature due to the deformation of the elastic medium, and therefore, the opposite effect of the deformation is due to the thermal state of the medium considered. The approximation of an infinite velocity of thermal disturbance represented by the parabolic form of the equation, as given in classical theory, does not represent a real quality, especially in problems related to heat shocks.

Generalised Thermoelastic theories give a modified version of the traditional Fourier's law of heat conduction, but also gives a hyperbolic heat equation for thermal pulses with finite velocities. According to these principles, thermal propagation is a wave phenomenon (not a diffusion phenomenon). Maxwell originally published in hyperbolic form (called the second sound).

The field of thermoelastic theories has undergone substantial progress over the years, resulting in multiple models, including coupled, uncoupled, and generalized thermoelasticity. The theoretical importance of thermoelasticity is strengthened by models such as the Lord-Shulman (L-S) model [1], Green-Lindsay (G-L) model [2], Green-Naghdi (G-N) model [3], Dual Phase Lag (DPL) model [4], Hetnarski-Ignaczak (H-I) model [5, 6], Chandrasekharaiah-Tzou (C-T) model [4, 7, 8], and Three Phase Lag model [9, 10]. [11, 12] declared results in the support of the DPL heat conduction model.

The nonlocal theory of Eringen [13, 14], as discussed in multiple research papers [15, 16, 17, 18], is a theoretical framework used to analyze the mechanical behavior of materials at the nanoscale level. The dependency of the stresses at a particular point in the region of a continuum body is not only on the strains at that point but also on the strains at all its surrounding points. This theory incorporates small-scale effects that become significant in micro-nanoscale structures, allowing for a more accurate representation of material properties. The nonlocal nature of these systems allows the analysis of microscopic effects at a macroscopic level, providing a deeper understanding of thermal behavior and wave propagation in various materials [19].

Various problems of inclined loads in thermoelastic media are discussed to better under-

stand material's behavior. Said [20] explored how rotation, inclined load, nonlocal effects, and a material constant influence key physical properties of a fiber-reinforced thermoelastic medium. [21] focused on two-dimensional deformation in a transversely isotropic thermoelastic diffusion medium. It examines the combined effects of diffusion, thermal influences, and inclination load, represented as a mixture of normal and tangential forces. [22] investigated a poro-thermoelastic half-space with temperature-dependent properties under an inclined load, using the three-phase delay model. It also considers the influences of magnetic and gravitational fields on the system.

This paper studies the effect of the oblique load on the plane wave in the nonlocal thermoelastic three-phase lag model. The variables under consideration are derived using analysis techniques. The effects of inclined angle on different physical quantities in non-local thermoelastic media are shown by plotting comparative plots.

2 Mathematical Framework

Stress-strain-temperature relation [16, 23]:

$$\sigma_{ij} = (1 - e_1^2\nabla^2)\sigma_{ij}^L = \mu(u_{j,i} + u_{i,j}) + (\lambda u_{r,r} - \gamma_1\vartheta)\delta_{ij}, \tag{2.1}$$

Displacement equation of motion without body forces [23]:

$$(\lambda + \mu)\nabla(\nabla.\overrightarrow{u}) - \gamma_1\nabla\vartheta + \mu\nabla^2\overrightarrow{u} = \rho(1 - e_1^2\nabla^2)\frac{\partial^2 u}{\partial t^2}, \tag{2.2}$$

Heat equation without considering heat sources [24]:

$$K^*\nabla^2\vartheta + \tau_v^*\nabla^2\vartheta_{,t} + K\tau_T\nabla^2\vartheta_{,tt} = (1 + \tau_q\frac{\partial}{\partial t} + \frac{\tau_q^2}{2}\frac{\partial^2}{\partial t^2})(\rho C_E\vartheta_{,tt} + T_0\gamma_1 u_{i,itt}), \tag{2.3}$$

Where σ_{ij}, σ_{ij}^L are nonlocal and local components of stress tensors. ϑ, T_0, K and K^* are the medium temperature in the natural state, the absolute temperature, the thermal conductivity and the additional material constant, respectively. $\tau_v^* = K + K^*\tau_v$. C_E is the specific heat at constant strain. ϑ is a temperature above the reference temperature T_0 such that $|\vartheta/T_0| << 1$. τ_T, τ_v, and τ_q are phase lags for temperature gradient, thermal displacement gradient, and heat flux, respectively. λ and μ are Lame's constants. ρ represents the density of the medium. u_i are displacement vector components and e is the cubical dilation. $,t$ represents time derivative and δ_{ij} is the Kronecker delta function.

3 Problem formulation

Following [25], consider a two-dimensional half-space ($z \geq 0$) for a homogeneous isotropic nonlocal thermoelastic medium. The origin is taken randomly on a flat surface, considering the positive direction of the z axis as vertical downward on the surface of the half-space y = 0. (Figure 1). In this study, directional components of displacement $\overrightarrow{u}$ are considered rectangular cartesian coordinates as in the following equation

$$u = u_x, v = v_y = 0, w = u_z. \tag{3.1}$$

Constitutive equations can be written as

$$\sigma_{xx} = (1 - e_1^2\nabla^2)\sigma_{xx}^L = 2\mu(\frac{\partial u}{\partial x}) + \lambda e - \gamma_1\vartheta, \tag{3.2}$$

$$\sigma_{zz} = (1 - e_1^2\nabla^2)\sigma_{zz}^L = 2\mu(\frac{\partial w}{\partial z}) + \lambda e - \gamma_1\vartheta, \tag{3.3}$$

$$\sigma_{xz} = (1 - e_1^2\nabla^2)\sigma_{xz}^L = \mu(\frac{\partial u}{\partial z} + \frac{\partial w}{\partial x}). \tag{3.4}$$

Using equations (3.2), (3.3), (3.4) equation (2.2) reduces to:

$$(\lambda + \mu)\frac{\partial e}{\partial x} + \mu\nabla^2 u - \gamma_1\frac{\partial\vartheta}{\partial x} = \rho(1 - e_1^2\nabla^2)\frac{\partial^2 u}{\partial t^2}, \tag{3.5}$$

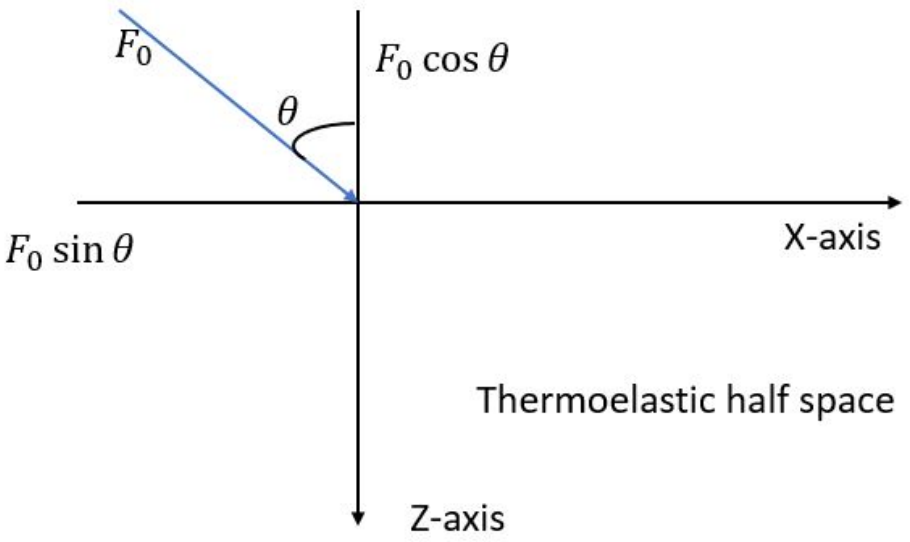

Figure 1. Tangential and Normal components of mechanical load over a nonlocal thermoelastic half-space

$$(\lambda+\mu)\frac{\partial e}{\partial z}+\mu\nabla^2 w-\gamma_1\frac{\partial \vartheta}{\partial z}=\rho(1-e_1^2\nabla^2)\frac{\partial^2 w}{\partial t^2}. \tag{3.6}$$

Applying the following relations of non-dimensional quantities for simplicity:

$$(t',\tau_T',\tau_v'\tau_q')=\Re(t,\tau_T,\tau_v,\tau_q),\ \ (x',z')=\frac{\Re}{c_1}(x,z),$$
$$(u',w')=\frac{\rho_1}{\beta_1 T_0}(u,w),\ \ \sigma_{ij}'=\frac{\sigma_{ij}}{\gamma_1 T_0},\ \vartheta'=\frac{\vartheta}{T_0},$$
$$\gamma_1=(3\lambda+2\mu)\alpha_t,\ \Re=\frac{\rho C_E c_1^2}{K},\ c_1^2=\frac{\lambda+2\mu}{\rho}.$$

Equations (2.3), (3.5), and (3.6) reduce to the following (Dashed lines are ignored to avoid complexity)

$$(\lambda+\mu)\frac{\partial e}{\partial x}+\mu\nabla^2 u-\rho c_1^2\frac{\partial \vartheta}{\partial x}=\rho c_1^2(1-e_1^2\nabla^2)\frac{\partial^2 u}{\partial t^2}, \tag{3.7}$$

$$(\lambda+\mu)\frac{\partial e}{\partial z}+\mu\nabla^2 w-\rho c_1^2\frac{\partial \vartheta}{\partial z}=\rho c_1^2(1-e_1^2\nabla^2)\frac{\partial^2 w}{\partial t^2}, \tag{3.8}$$

$$\begin{aligned}&K^*\nabla^2\vartheta+(K\Re+K^*\tau_v)\nabla^2\vartheta_{,t}+K\Re\tau_T\nabla^2\vartheta_{,tt}\\&=(1+\tau_q\frac{\partial}{\partial t}+\frac{\tau_q^2}{2}\frac{\partial^2}{\partial t^2})(\rho c_1^2 C_E\vartheta_{,tt}+\frac{T_0\gamma_1^2}{\rho}u_{i,itt}).\end{aligned} \tag{3.9}$$

Displacement components can be written using displacement potentials by using Helmholtz decomposition:

$$u=\frac{\partial q}{\partial x}+\frac{\partial \psi}{\partial z}, w=\frac{\partial q}{\partial z}-\frac{\partial \psi}{\partial x}, e=\nabla^2 q, \nabla^2\psi=\frac{\partial u}{\partial z}-\frac{\partial w}{\partial x}, \tag{3.10}$$

where, q and ψ functions of (x, z, t) are scalar and vector potential functions, respectively. Substituting (3.10) into (3.7), (3.8), (3.9).

$$(\nabla^2 - (1 - e_1^2\nabla^2)\frac{\partial^2}{\partial t^2})q - \vartheta = 0, \tag{3.11}$$

$$(a_1\nabla^2 - (1 - e_1^2\nabla^2)\frac{\partial^2}{\partial t^2})\psi = 0, \tag{3.12}$$

$$\begin{aligned} &K^*\nabla^2\vartheta + (K\Re + K^*\tau_v)\nabla^2\vartheta_{,t} + K\Re\tau_T\nabla^2\vartheta_{,tt} \\ &= (1 + \tau_q\frac{\partial}{\partial t} + \frac{\tau_q^2}{2}\frac{\partial^2}{\partial t^2})(\rho c_1^2 C_E\vartheta_{,tt} + \frac{T_0\gamma_1^2}{\rho}\nabla^2 q). \end{aligned} \tag{3.13}$$

4 Solution of the problem

Following [25] variables' solution under consideration using the normal mode approach is

$$(q, \psi, \vartheta)(x, z, t) = (\tilde{q}, \tilde{\psi}, \tilde{\vartheta})(z)e^{\iota(ax-bt)}, \tag{4.1}$$

where all the functions with˜signs on the right-hand side represent the function amplitude, b is the complex constant, and a represent the wave number along the X-axis. Substituting the solutions (4.1) into equations (3.11), (3.12), (3.13), we get two coupled and one uncoupled differential equations as follows:

$$(O_1D^2 - O_2)\tilde{q} - \tilde{\vartheta} = 0, \tag{4.2}$$

$$(O_3D^2 - O_4)\tilde{\psi} = 0, \tag{4.3}$$

$$(O_5D^2 - O_6)\tilde{\vartheta} - (O_{13}D^2 - O_7)\tilde{q} = 0, \tag{4.4}$$

where, $D = \frac{d}{dz}$,

$$O_1 = 1 - e_1^2b^2,\ O_2 = a^2 - b^2 - e_1^2a^2b^2,\ O_3 = a_1 - e_1^2b^2,\ O_4 = a^2a_1 - b^2 - a^2e_1^2b^2,$$
$$O_5 = K^* + O_9 + O_{10},\ O_6 = a^2(K^* + O_9 + O_{10}) - (O_{11}O_{12}),\ O_8 = -\frac{b^2\gamma_1^2T_0}{\rho},$$
$$O_7 = -(a^2O_{11}O_8),\ O_9 = -b(K\Re + K^*\tau_v)i,\ O_{10} = -b^2K\Re\tau_T,\ O_{13} = O_{11}O_8,$$
$$O_{11} = 1 - b\tau_q i - \frac{b^2\tau_q^2}{2},\ O_{12} = -\rho c_1^2C_Eb^2.$$

Solving the non-trivial solution of homogeneous equations (4.2), (4.3), and (4.4), for three variables $(\tilde{q}, \tilde{\psi}, \tilde{\vartheta})$, the following fourth-order differential equation is obtained by making determinant of coefficients equal to zero, which further is solved to get k_i^2 $(i = 1, 2)$ as roots of the following equation:

$$(D^4 + L_1D^2 + L_2)(\tilde{q}, \tilde{\vartheta}) = 0 \tag{4.5}$$

where,

$$V_1 = -O_1O_5,\ V_2 = O_{13} + O_2O_5 + O_6O_1,\ V_3 = -(O_7 + O_2O_6),$$
$$L_1 = \frac{V_2}{V_1},\ L_2 = \frac{V_3}{V_1},\ k_3^2 = O_4/O_3.$$

The solutions of the differential equation (4.5), as $z \to \infty$

$$(\tilde{q}_{(r=0)}, \tilde{\vartheta}_{(r=1)}, \tilde{\psi}_{(r=2)})(z) = \sum_{n=1}^{3} E_{rn}M_n(a, b)e^{-k_nz}, \tag{4.6}$$

where,

$$E_{11} = \frac{(O_{13}k_1^2 - O_7)}{(O_5 k_1^2 - O_6)}, E_{12} = \frac{(O_{13}k_2^2 - O_7)}{(O_5 k_2^2 - O_6)},$$
$$E_{01} = E_{02} = E_{23} = 1, E_{03} = E_{13} = E_{21} = 0 = E_{22}.$$

Stresses can be represented using non-dimensional quantities and using equation (3.10), as:

$$\sigma_{zz} = (1 + P_1)\frac{\partial^2 q}{\partial z^2} - P_1 \frac{\partial^2 \psi}{\partial z \partial x} + \frac{\partial^2 q}{\partial x^2} - \vartheta, \tag{4.7}$$

$$\sigma_{zx} = a_1 (2\frac{\partial^2 q}{\partial z \partial x} - \frac{\partial^2 \psi}{\partial x^2} + \frac{\partial^2 \psi}{\partial z^2}), \tag{4.8}$$

where,

$$a_1 = \frac{\mu}{\rho c_1^2}, \ P_1 = \frac{1}{\rho c_1^2}.$$

Applying normal mode analysis and displacement components, equations (3.3), (3.4) and (2.1) yield the following:

$$\tilde{\sigma}_{zz} = ((1 + P_1)D^2 - a^2)\tilde{q} + \iota a P_1 D\tilde{\psi} - \tilde{\vartheta}, \tag{4.9}$$

$$\tilde{\sigma_{zx}} = a_1[2\iota a D\tilde{q} + (D^2 - a^2)]\tilde{\psi}, \tag{4.10}$$

$$\tilde{w} = D\tilde{q} - \iota a\tilde{\psi}, \ \ \tilde{u} = \iota a\tilde{q} + D\tilde{\psi}. \tag{4.11}$$

Using solutions (4.6), equations (4.9), (4.10), (4.11) can be expressed as:

$$\tilde{\sigma}_{zz(r=3)} = \sum_{n=1}^{2} E_{3n} M_n(a, b) e^{-k_n z} + E_{33} M_3 e^{-k_3 z}, \tag{4.12}$$

$$\tilde{\sigma}_{zx(r=4)} = \sum_{n=1}^{2} E_{4n} M_n e^{-k_n z} + E_{43} M_3 e^{-k_3 z}, \tag{4.13}$$

$$\tilde{u}_{(r=5)} = \sum_{n=1}^{2} E_{5n} M_n(a, b) e^{-k_n z} + E_{53} M_3 E_{23} e^{-k_3 z}, \tag{4.14}$$

$$\tilde{w}_{(r=6)} = \sum_{n=1}^{2} E_{6n} M_n(a, b) e^{-k_n z} + E_{63} M_3 e^{-k_3 z}, \tag{4.15}$$

where,

$$E_{3n} = -a^2 + (1 + P_1)k_n^2 - E_{1n}, \ E_{33} = P_1 i a k_3 E_{23},$$
$$E_{4n} = -2a_1 i a k_n, \ E_{43} = E_{23} a_1 (k_3^2 + a^2),$$
$$E_{5n} = E_{63} = -ia, \ E_{53} = -k_3, \ E_{6n} = -k_n.$$

5 Application of inclined load

The boundary conditions are subject to inclined load F_0 at a particular angle θ with the Z-axis (Figure 1), and its component along the X-axis is $F_0 \sin\theta$ and along the Z-axis is $F_0 \cos\theta$.

$$\tilde{\sigma}_{zz} = -F_0 \cos\theta,\ \tilde{\sigma}_{zx} = -F_0 \sin\theta,\ \tilde{\vartheta} = 0. \tag{5.1}$$

Equations (4.12), (4.13), and (4.6), for r = 1, after applying the above-mentioned mechanical boundary conditions, transform to the following non-homogeneous set of equations.

$$\begin{bmatrix} E_{11} & E_{12} & E_{13} \\ E_{31} & E_{32} & E_{33} \\ E_{41} & E_{42} & E_{43} \end{bmatrix} \begin{bmatrix} M_1 \\ M_2 \\ M_3 \end{bmatrix} = \begin{bmatrix} 0 \\ R_1 \\ R_2 \end{bmatrix} \tag{5.2}$$

where,

$$R_1 = -F_0 \cos\theta, R_2 = -F_0 \sin\theta.$$

The solution of the above set of equations is generated using Cramer's rule.

$$M_n = \frac{\Delta_n}{\Delta}; n = 1, 2, 3. \tag{5.3}$$

Using the above solutions, equations (4.6), (4.12), (4.13), (4.14), (4.15) lead to

$$\begin{aligned} &(\tilde{\psi}_{(r=2)}, \tilde{q}_{(r=0)}, \tilde{\sigma}_{zx(r=4)}, \tilde{\sigma}_{zz(r=3)}, \tilde{u}_{(r=5)}, \tilde{w}_{(r=6)}, \tilde{\vartheta}_{(r=1)})(z) \\ &= \frac{1}{\Delta} \sum_{n=1}^{3} \Delta_n E_{rn} e^{-k_n z}. \end{aligned} \tag{5.4}$$

6 Numerical discussions

To show the contribution of mechanical load at different inclined angles on the variation of different parameters, the following physical constants of magnesium crystal-like material [25] are considered for numerical computations.

$$\begin{aligned} &T_0 = 298\,\text{K}, \quad \lambda = 9.4 \times 10^{10}\,\text{N m}^{-2}, \quad \mu = 4.0 \times 10^{10}\,\text{N m}^{-2}, \\ &\rho = 1.74 \times 10^3\,\text{kg/m}^3,\ \gamma_1 = 0.779 \times 10^{-9}\,\text{N}, \quad C_E = 1.04 \times 10^3\,\text{kg m}^{-3}, \\ &K = 1.7 \times 10^2\text{J m}^{-1}\text{s}^{-1}\text{deg}^{-1}, \quad K^* = 1.0 \times 10^2\text{J m}^{-1}\text{s}^{-1}\text{deg}^{-1}, \\ &\alpha_t = 7.4033 \times 10^{-7}\,\text{K}^{-1}, \quad F_0 = 1, a = 3.8, \quad b = b_0 + ib_1, \\ &b_0 = 2.5\,\text{rad/s}, \quad b = 0.3\,\text{rad/s}, \quad e_1 = 0.09. \end{aligned}$$

The angular velocity b present in the term $e^{\iota(ax-bt)}$ can be expressed as a complex number. Only the real part is considered for small values of time (t). The above values for calculating variation in field variables are graphically represented. Graphs express the different parameters against distance at three different values of inclined angle. Considering values of $\theta = 0, \theta = 45$, and $\theta = 60$, three different colored curves are represented as black, red, and blue, respectively. Results are represented graphically at different positions of z as $(0 \le z \le 4)$ at $t = 0.1$ and $x = 0.3$.

Figure 2-3 shows the spatial variation of potentials q and ψ against distance z as $(0 \le z \le 4)$ for different inclined angles of mechanical load. For $\theta = 0$, when load F_0 is applied along the z-axis, the values of q decrease as z increases initially and gradually become zero after $z = 0.8$.

Figure 2 shows the reverse behavior of the potential q with an angular value of 60 and approaches zero as z increases after a particular value of 0.8. It shows a significant effect of θ on q.

Figure 3 depicts the impact of the inclined angle on the variation of potential ψ against distance.

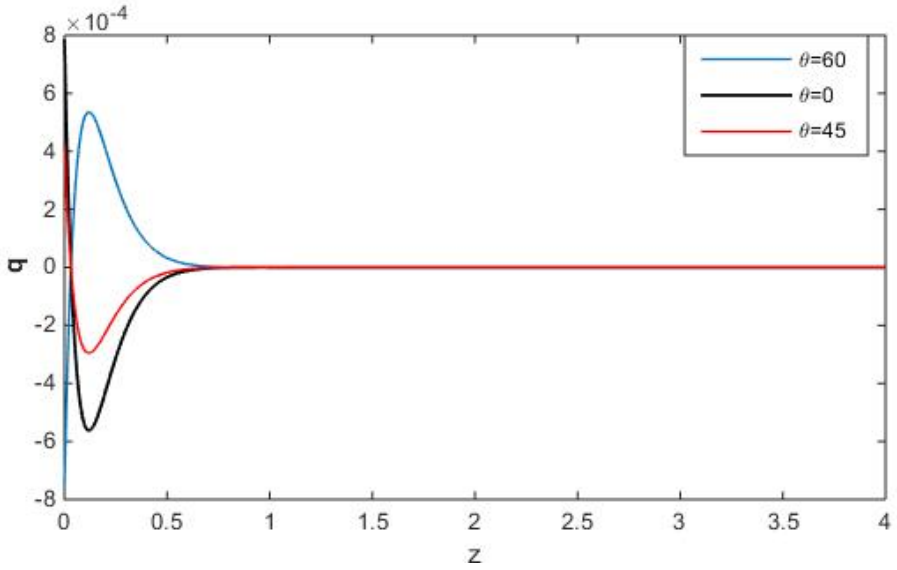

Figure 2. Variation of potential q against z

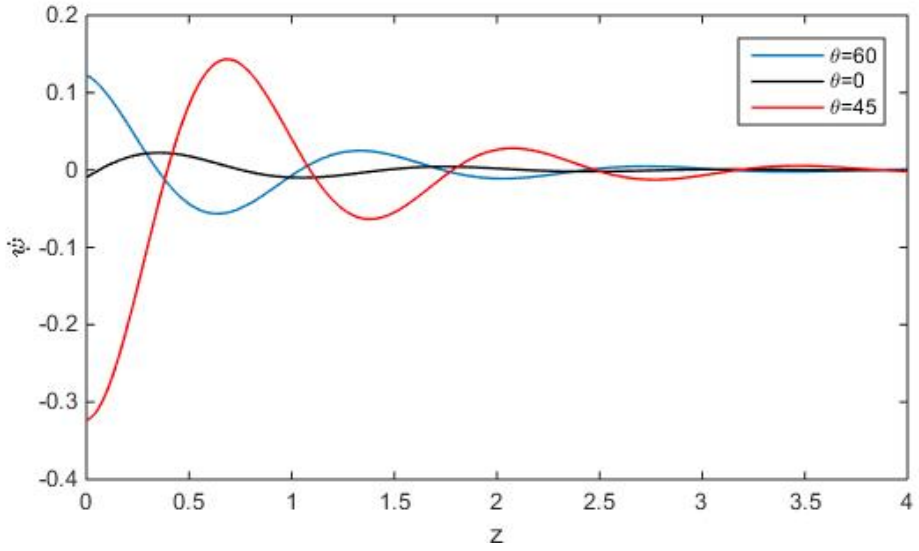

Figure 3. Variation of potential ψ against z

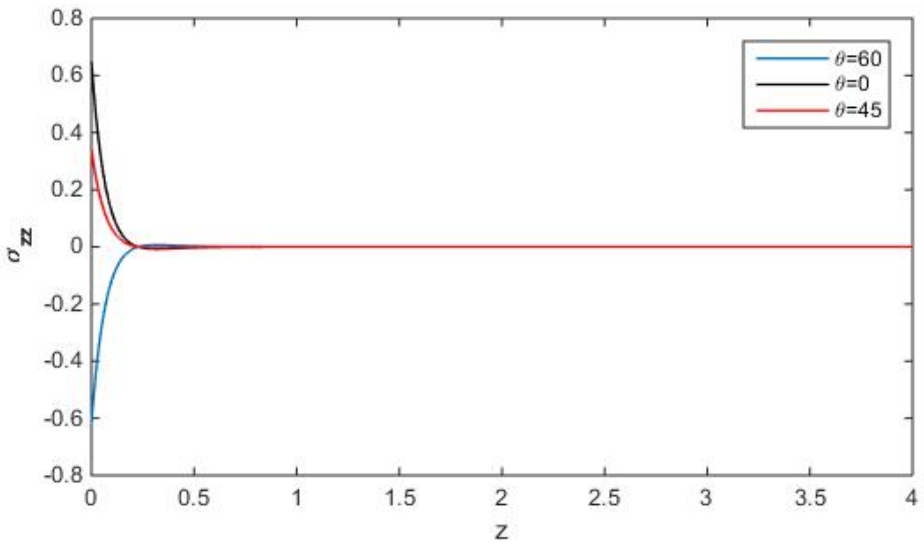

Figure 4. Variation of Normal stress against z

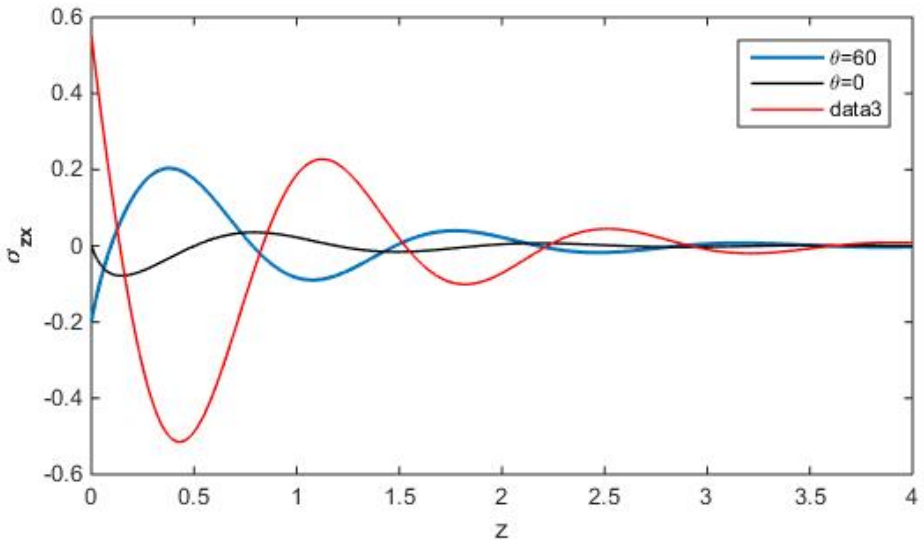

Figure 5. Variation of Tangential stress against z

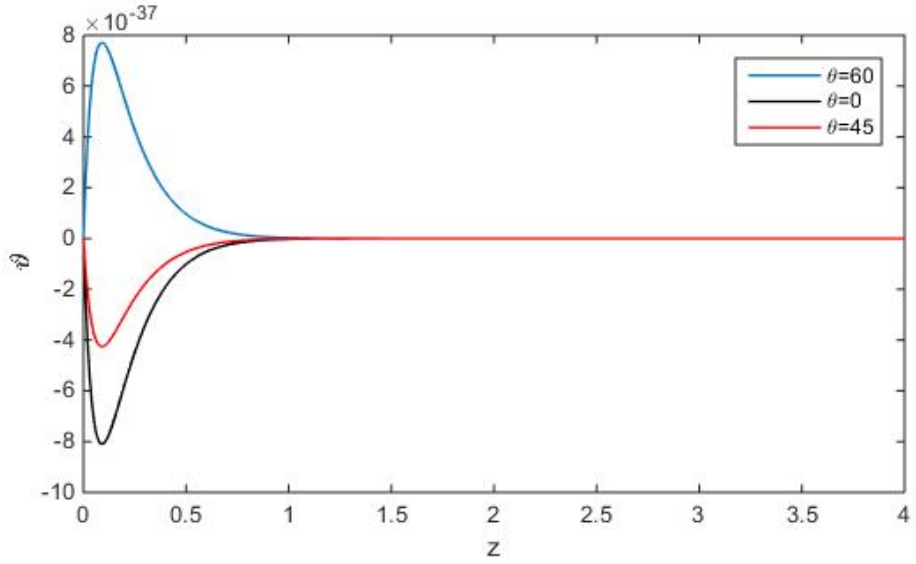

Figure 6. Variation of temperature against z

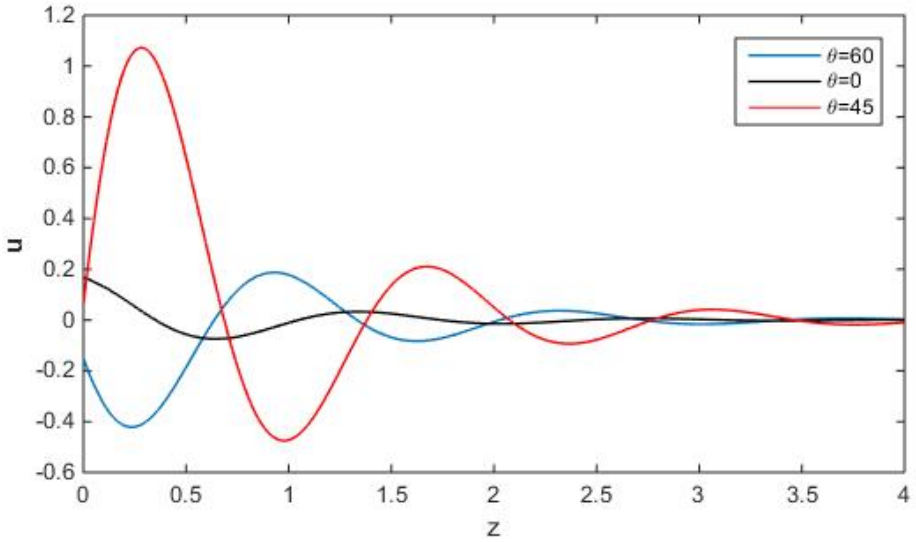

Figure 7. Variation of displacement u against z

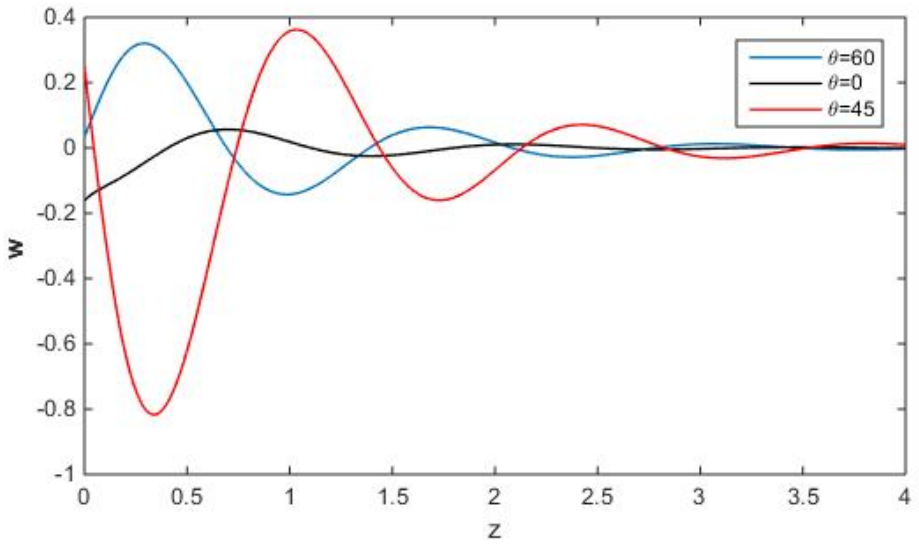

Figure 8. Variation of displacement w against z

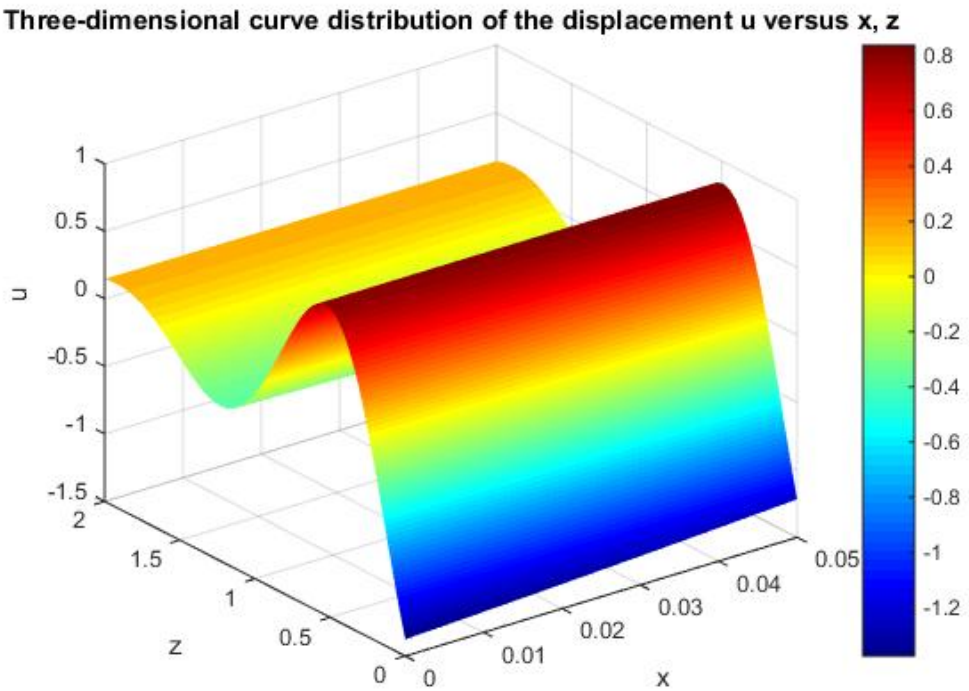

Figure 9. Variation of displacement u against x,z

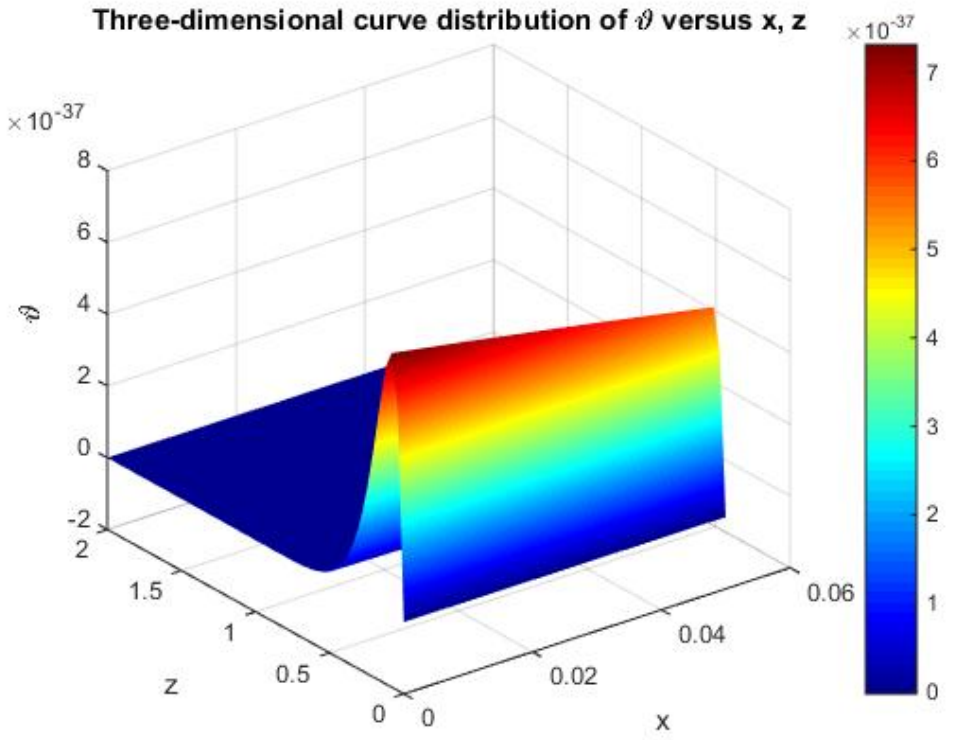

Figure 10. Variation of temperature against x,z

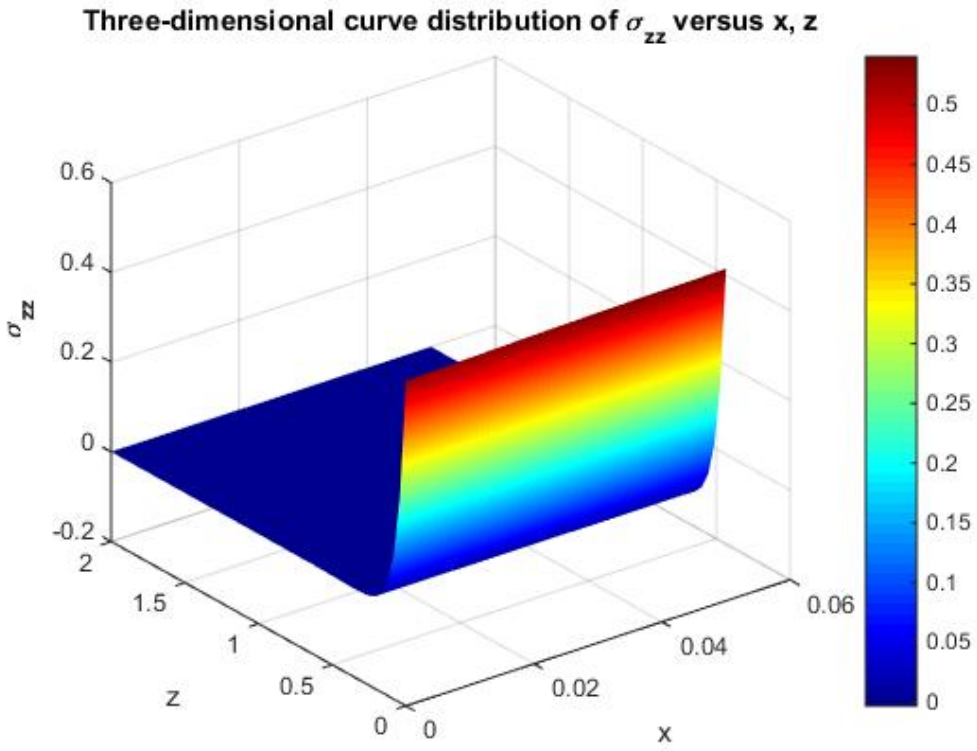

Figure 11. Variation of normal stress against x,z

Fluctuations in a variation of ψ can be seen with different values of θ, and then after $z = 3$ amplitude goes to zero for all values of θ.
Figure 4 represents the variation of normal stress along the distance. The maximum impact in normal stress can be seen as z varies from 0 to 0.3 (i.e. $0 \leq z \leq 0.3$) and becomes zero afterward for all considered values of θ. The behavior of the normal component of stress is same for $\theta = 0$ and 45. For $\theta = 60$ the values of σ_{zz} increase from negative to zero with increase of z.
Figure 5 illustrates the influence of the angle of inclination on the variability of tangential stress along distance z. The starting point of the curve with different values of θ is different. The tangential stress component does not show noticeable variation for $\theta = 0$, decreases first, and then becomes constant in the case of zero initial stress,s and an opposite variation is observed with initial stress. Variation in amplitude can be observed with $\theta = 45$ and 60. In the case of $\theta = 45$, the value of σ_{zx} decreases from 0.6 to negative values and shows a damped wave type of behavior as z increases.
Figure 6 shows the impact of varied inclined angles on temperature along distance. The temperature field has a coincident starting point of zero magnitude for all three cases. With the change of angle of inclination of the applied load, temperature variation can be seen. At angle $\theta = 60$, the temperature rises with an increase of z up to z = 0.1, and after a particular maximum value, it decreases to zero and remains zero after z = 1. The same variation in temperature is observed but in the opposite direction (up to z = 0.1) for $\theta = 0$. Variation in θ is in the specified range of z $(0 \leq z \leq 1)$.
Figure 7 influences of varied angles on thermodynamic displacement component u against distance. At $z = 0$, the starting point andvior of all three curves are not the same. A damping wave-like motion of curves is observed. At $\theta = 0$ amplitude variation of the curve is almost negligible. After z = 3, all the curves with different angles of inclination become almost constant and approach zero.
Figure 8 shows the impact of inclined load on displacement component w along the distance. Noticeable variation of amplitudes in the opposite direction is observed as $\theta = 45$ and 60, whereas variation is not significant in the case of $\theta = 0$. All three curves start with different initial points at z = 0. and show the same steady-state behavior after z = 3.
Figures 9-11 are three-dimensional curves of displacement u, temperature ϑ, and normal stress at an angle of inclination $\theta = 45$. These curves are important for understanding the variation of physical quantities along the downward vertical component of distance. Dependency on the nature of applied mechanical forces can be studied and compared more closely with 3D visualization of curves.

7 Special Case

CaseI: Neglecting the effect of nonlocality $(e_1 = 0)$, the results of the present problem coincide with those obtained by [25] in the absence of initial stress.
Case II: When $K^* = 0$, Equation (2.3) simplifies to Equation (7.7) from [8], which pertains to the dual-phase lag model in thermoelasticity.
CaseIII: Effect of nonlocality with oblique load can be represented by the above set of equations under the L-S model of thermoelasticity (see [24]) by setting $tau_T = 0$, $\tau_q^2 = 0$, $\tau_\vartheta = 0$ and $K^* = 0$ $(\tau_\vartheta^* = K)$.

8 Conclusion

The analytical solutions of an interesting solid mechanics problem have been calculated to observe the temperature distribution, displacement components, and normal and tangential stresses under the applied mechanical load. The influence of inclined load on a non-local generalized thermoelastic half-space is compared at different angles of inclination. Following are the concluding points:
(1) Exact solutions for the thermoelastic problem in solids have been calculated using the Normal mode analysis method and applied effectively.
(2) In the graphs, all fields are varied in a limited region, which supports the physical facts and notion of generalized thermoelasticity theory.

(3) A significant effect of the angle of inclination of the load is observed in all the considered fields (Figure 2-8).
(4) Different patterns of variation are observed for different values of the angle of inclination on physical fields.
(5) As intended, all physical quantities meet the boundary conditions and are continuous. The deforming behavior of the solid medium under consideration has a dependency on the nature of acting forces and imposed boundary conditions. As the value of z increases, all the physical quantities under study approach zero.
The significance of this problem becomes apparent when considering the actual behavior of materials with the appropriate model. Valuable materials, such as oils exist in crude form within the Earth, while the rocks or materials surrounding them are often granular. The crude fluids and granular rocks can be effectively modeled using the micropolar theory of thermoelasticity. This field finds applications in seismology, geomechanics, earthquake engineering, and related areas.

References

[1] H.W. Lord and Y. Shulman, *A generalized dynamical theory of thermoelasticity*, Journal of the Mechanics and Physics of Solids, Vol. 15, No. 5, pp. 299–309 (1967).

[2] A.E. Green and K.A. Lindsay, *Thermoelasticity*, Journal of Elasticity, Vol. 2, No. 1, pp. 1–7 (1972).

[3] A.E. Green and P.M. Naghdi, *Thermoelasticity without energy dissipation*, Journal of Elasticity, Vol. 31, No. 3, pp. 189–208 (1993).

[4] D.Y. Tzou, *A unified field approach for heat conduction from macro-to micro-scales*, Journal of Heat Transfer, Vol. 117, No. 1, pp. 8–16 (1995).

[5] R.B. Hetnarski and J. Ignaczak, *Soliton-like waves in a low temperature nonlinear thermoelastic solid*, International Journal of Engineering Science, Vol. 34, No. 15, pp. 1767–1787 (1996).

[6] R.B. Hetnarski and J. Ignaczak, *Soliton-like waves in a low-temperature nonlinear rigid heat conductor*, International Journal of Engineering Science, Vol. 33, No. 12, pp. 1725–1741 (1995).

[7] D.S. Chandrasekharaiah, *A uniqueness theorem in the theory of thermoelasticity without energy dissipation*, Journal of Thermal Stresses, Vol. 19, No. 3, pp. 267–272 (1996).

[8] D.S. Chandrasekharaiah, *Hyperbolic thermoelasticity: a review of recent literature*, Applied Mechanics Reviews, Rev., vol. 51, no. 12, Pt. I, (1998).

[9] R. Quintanilla and R. Racke, *A note on stability in three-phase-lag heat conduction*, International Journal of Heat and Mass Transfer, Vol. 51, No. 1–2, pp. 24–29 (2008).

[10] M. Singh and S. Kumari, *Developments in theory of thermoelasticity*, Union of Researchers of Macedonia, Vol. 9, No. 8, pp. 5537–5547 (2020).

[11] R. Quintanilla and R. Racke, *A note on stability in dual-phase-lag heat conduction*, International Journal of Heat and Mass Transfer, Vol. 49, No. 7–8, pp. 1209–1213 (2006).

[12] L. Wang and M. Xu, *Well-posedness of dual-phase-lagging heat conduction equation: higher dimensions*, International Journal of Heat and Mass Transfer, Vol. 45, No. 5, pp. 1165–1171 (2002).

[13] A.C. Eringen and D.G.B. Edelen, *On nonlocal elasticity*, International Journal of Engineering Science, Vol. 10, No. 3, pp. 233–248 (1972).

[14] A.C. Eringen, *Linear theory of nonlocal elasticity and dispersion of plane waves*, International Journal of Engineering Science, Vol. 10, No. 5, pp. 425–435 (1972).

[15] M. Shaat, E. Ghavanloo and S.A. Fazelzadeh, *Review on nonlocal continuum mechanics: physics, material applicability, and mathematics*, Mechanics of Materials, Vol. 150, Article ID 103587 (2020).

[16] K.K. Kalkal, D. Sheoran and S. Deswal, *Reflection of plane waves in a nonlocal micropolar thermoelastic medium under the effect of rotation*, Acta Mechanica, Vol. 231, pp. 2849–2866 (2020).

[17] D. Kumar, D. Singh, S.K. Tomar, S. Hirose, T. Saitoh and A. Furukawa, *Waves in nonlocal elastic material with double porosity*, Archive of Applied Mechanics, Vol. 91, pp. 4797–4815 (2021).

[18] S. Sharma and S. Kumari, *Reflection of Plane Waves in Nonlocal Fractional-Order Thermoelastic Half Space*, International Journal of Mathematics and Mathematical Sciences, Vol. 2022, No. 1, Article ID 1223847 (2022).

[19] M.I.A. Othman, S.M. Said and M. Eldemerdash, *The effect of nonlocal on poro-thermoelastic solid with dependent properties on reference temperature via the three-phase-lag model*, Journal of Materials and Applications, Vol. 12, No. 1, pp. 21–30 (2023).

[20] S.M. Said, *The impact of rotation and inclined load on a nonlocal fiber-reinforced thermoelastic half-space via simple-phase-lag model*, Journal of Vibration Engineering & Technologies, pp. 1–10 (2024).

[21] P. Lata et al., *Thermomechanical interactions in a transversely isotropic thermoelastic media with diffusion due to inclined load*, Structural Engineering and Mechanics, Vol. 90, No. 3, pp. 263–272 (2024).

[22] S.M. Said, *The effect of magnetic field and inclined load on a poro-thermoelastic medium using the three-phase-lag model*, Geomechanics and Engineering, Vol. 37, No. 3, pp. 243 (2024).

[23] A.E. Abouelregal, H. Mohammad-Sedighi, A.H. Shirazi, M. Malikan and V.A. Eremeyev, *Computational analysis of an infinite magneto-thermoelastic solid periodically dispersed with varying heat flow based on non-local Moore–Gibson–Thompson approach*, Continuum Mechanics and Thermodynamics, Vol. 34, No. 4, pp. 1067–1085 (2022).

[24] S.K. Roy Choudhuri, *On a thermoelastic three-phase-lag model*, Journal of Thermal Stresses, Vol. 30, No. 3, pp. 231–238 (2007).

[25] M.I. Othman, E.M. Abd-Elaziz and A.E. Younis, *Effect of inclined load and initial stress on plane waves of thermoelastic rotating medium via three-phase-lag model*, Mechanics of Solids, Vol. 58, No. 9, pp. 3333–3345 (2023).

Author information

S. Bajaj, Department of Mathematics, Maharishi Markandeshwar (Deemed to be University), Mullana, Ambala, Haryana, India.
Department of Mathematics, Chandigarh University, Mohali, Punjab, India.
E-mail: bajajsonia1501@gmail.com

A. K. Shrivastav, Department of Mathematics, Maharishi Markandeshwar (Deemed to be University) Mullana, Ambala, Haryana, India.
E-mail: aakkaasshhkumar8888@gmail.com

S. Kumari, Department of Mathematics, Chandigarh University, Mohali, Punjab, India.
E-mail: sangwan.sangeeta.ss@gmail.com